Egyptian Journal of Radiology and Nuclear Medicine

RESEARCH

Open Access

Evaluation of high temporal resolution magnetic resonance imaging of the liver with gadoxetate disodium in combination with compressed sensing and parallel imaging under single breath-holding using a 1.5-T magnetic resonance system

Fumiaki Fukamatsu[1], Akira Yamada[1*], Ayumi Sakai[1], Marika Shimizu[1], Fumihito Ichinohe[1], Masaaki Takahashi[1], Hayato Hayashihara[2], Yoshihiro Kitou[2] and Yasunari Fujinaga[1]

Abstract

Background This study aimed to determine the optimal scan time for high temporal resolution magnetic resonance (MR) imaging of the liver with gadoxetate disodium injection in combination with compressed sensing (CS) and parallel imaging (PI) techniques under single breath-holding using a 1.5-T MR system.

Methods Sixty-two participants underwent multiple arterial phases of dynamic contrast-enhanced magnetic resonance imaging (DCE-MRI) of the liver with gadoxetate disodium using fat-suppressed GRE T1-weighted imaging—liver acquisition with volume acceleration (LAVA)—in combination with CS and PI using a 1.5-T MR system. Forty-six and 22 participants underwent 6-s and 10-s scans, respectively. Pre-contrast, multiple arterial, portal venous, and hepatobiliary phase images were acquired. Two radiologists evaluated the visual scores for the outline of the liver, inferior right hepatic vein (IRHV), right portal vein, right hepatic artery, appropriateness of the arterial phase, and overall image quality using a 4- or 5-point scale.

Results The overall image quality and the image quality of the outline of the liver in the pre-contrast and arterial phases and IRHV in the pre-contrast phase were significantly better ($P < 0.05$) in the 10-s scan group than those in the 6-s scan group. No significant difference was observed between the two groups in terms of the appropriateness of the arterial phase (obtaining the optimal arterial phase) ($P = 0.731$).

Conclusions A 10-s scan protocol is recommended for high temporal resolution DCE-MRI of the liver with gadoxetate disodium injection in combination with CS and PI under single breath-holding using a 1.5-T MR system.

Keywords Compressed sensing, Gadoxetate disodium, Liver, Magnetic resonance imaging, Parallel imaging

*Correspondence:
Akira Yamada
a_yamada@shinshu-u.ac.jp
Full list of author information is available at the end of the article

Background

The acquisition of arterial phase images in optimal quality and timing plays a crucial role in the detection and diagnosis of hepatocellular carcinomas (HCCs) [1]. Multiple arterial phase dynamic contrast-enhanced magnetic resonance imaging (DCE-MRI) of the liver can be used to obtain optimal arterial phase images and for differentiating HCCs from hypervascular pseudolesions in patients with cirrhosis or chronic hepatitis [2–6]. A correlation has been observed between the intravenous bolus injection of gadoxetate disodium and severe motion artifacts associated with transient acute dyspnea during the arterial phase in gadoxetate disodium-enhanced liver MR imaging [7]. Multiple arterial phase acquisitions reduce the incidence of severe motion artifacts in the arterial phase following the intravenous bolus injection of gadoxetate disodium [5, 8, 9]. Thus, multiple arterial phase DCE-MRI of the liver is useful for the diagnosis of HCCs.

High temporal resolution MR imaging has reduced the data acquisition time for obtaining multiple arterial phase DCE-MRIs of the liver. Compressed sensing (CS) and parallel imaging (PI) are established techniques that are known to accelerate data acquisition. Several studies have evaluated the usefulness of these techniques, individually or in combination, in multiple arterial phase DCE-MRI of the liver [2, 4, 5]. One arterial phase must be acquired in 10 or 6.5 s to obtain a double or triple arterial phase under a single breath-holding time of 20 s. The usefulness of a scan time of 6.5 and 10 s in combination with CS and PI in 3-T MR systems has been reported [10, 11]. Liver acquisition with volume acceleration (LAVA) is a three-dimensional spoiled gradient-echo sequence used for DCE abdominal imaging with a high signal-to-noise ratio (SNR). The quality of the images acquired via 6-s and 10-s pre-contrast fat-suppressed gradient-echo T1-weighted imaging, i.e., LAVA, in combination with CS and PI under single breath-holding using a 1.5-T MR system, has been reported for healthy volunteers [12]. However, no study has determined whether a scan time of 6 or 10 s is optimal for high temporal resolution MR imaging of the liver with gadoxetate disodium in combination with CS and PI under single breath-holding in a 1.5-T MR system. The 1.5-T MR system has significant advantages over 3-T MR systems in the clinical setting. The 1.5-T MR system yields images with fewer metal and motion artifacts than the 3-T MR system. Furthermore, a large volume of ascites degrades the image quality in a 3-T MR system as the radiofrequency penetration declines and becomes non-uniform [13]. Consequently, it is important to establish an optimal high temporal resolution MR imaging protocol for the liver using a 1.5-T MR system.

Hence, this study aimed to determine the optimal scan protocol for high temporal resolution MR imaging of the liver with gadoxetate disodium in combination with CS and PI under single breath-holding using a 1.5-T MR system.

Methods

Participants

This study was approved by the Institutional Review Board of our institution, and written informed consent was obtained from all participants. The study population comprised consecutive patients who had undergone hepatic DCE-MRI with gadoxetate disodium injection under single breath-holding using a 1.5-T MR system between September 2017 and October 2018. Sixty-seven eligible participants were identified. The exclusion criteria included (1) an interval of > 3 months between the MRI examination and the last blood test, (2) a history of right hepatectomy, as the posterior segment of the liver was evaluated in this study, (3) portal venous thrombosis, (4) prominent arterioportal shunts, and (5) a large amount of ascites. The blood tests included platelet, total bilirubin, and albumin. The platelet count, total bilirubin levels, albumin levels, and albumin–bilirubin (ALBI) score and grade were assessed to evaluate the liver function of the participants. An interval between the MRI examination and the last blood test was set at 3 months to reflect liver function at the time of MRI examination. Five participants were excluded based on these criteria.

The MRI examinations were performed using two protocols according to scan time (10 s and 6 s). The MRI examinations according to each scan protocol were implemented for a defined period of 6 months. The participants who underwent DCE-MR examinations with 6-s scan between September 2017 and February 2018 were included in 6-s scan group, and ones with 10-s scan between May 2018 and October 2018 were included in 10-s scan group.

MR imaging

MR imaging was performed using a 1.5-T scanner (Optima MR450w; GE Healthcare, Waukesha, WI, USA) equipped with a 30-channel cardiac and spine coil. All images were acquired using LAVA in combination with CS (CS additional acceleration) and PI (auto-calibrating reconstruction for Cartesian imaging; ARC) under single breath-holding. The trajectory of the data sampling in k-space was Cartesian. Table 1 presents the scan parameters. The CS factor, phase ARC, and slice ARC in the 6-s scan group were 2.0, whereas the CS factor, phase ARC, and slice ARC were 2.0, 2.0, and 1.2, respectively, in the 10-s scan group. The acceleration factors for the 10-s scan were determined according to the results of a

Table 1 Scan parameters of the two groups

Parameter	6-s scan (triple arterial phase)	10-s scan (double arterial phase)
Field of view (mm^2)	320×320	320×320
Slice thickness (mm)	4	4
Matrix	256×192	256×192
Bandwidth (Hz/pixel)	488.281	488.281
Repetition time (msec)	5.546	5.546
Echo time (msec)	1.416	1.416
Flip angle (degree)	12	12
CS factor	2.0	2.0
Phase ARC	2.0	2.0
Slice ARC	2.0	1.2
Acquisition time (sec)	6	10

CS, compressed sensing, ARC, auto-calibrating reconstruction for Cartesian imaging

previous study [12]. The data acquisition time was the same for all phases in both groups. Multiple arterial phase acquisitions were obtained consecutively within a single breath-holding time of 20 s; thus, a triple arterial phase was acquired in the 6-s scan group, whereas a double arterial phase was acquired in the 10-s scan group.

After obtaining pre-contrast images, 0.025 mmol/kg (0.1 mL/kg) of gadoxetate disodium (Primovist; Bayer AG, Leverkusen, Germany) was administered with 50 mL of saline flush at a rate of 2 mL/s using a power injector (Sonic Shot GX or 7, NEMOTO, Japan). After initiating contrast material injection, multiple arterial, portal venous, and hepatobiliary phase MR imaging were performed at 15 s, 21 s, 27 s, 48 s, and 20 min in the 6-s scan group and 15 s, 25 s, 49 s, and 20 min in the 10-s scan group. Figure 1 illustrates the flowchart of the MR examinations performed in this study.

Quantitative image analysis

The multiple arterial and hepatobiliary phase MR images were evaluated. The regions of interest (ROIs) were drawn by a board-certified radiologist with 11 years of experience in abdominal imaging. The ROIs were placed at the location of the posterior segment of the right hepatic lobe, at the level of the posterior segmental branch of the portal vein. Large vessels were not included in the ROIs. The mean signal intensity (SI) and standard deviation (SD) within the ROIs were measured, and the SNR (mean SI/SD) of the liver was calculated [14–16]. All procedures were performed on clinical DICOM viewer (EV Insight; PSP Corporation, Tokyo, Japan).

Qualitative image analysis

Two board-certified radiologists with 9 and 14 years of experience in abdominal MR imaging evaluated the visualization of the following items using the visual score (VS) as part of qualitative image analysis: the outline of the liver; the inferior right hepatic vein (IRHV); the right portal vein (RPV); and the right hepatic artery

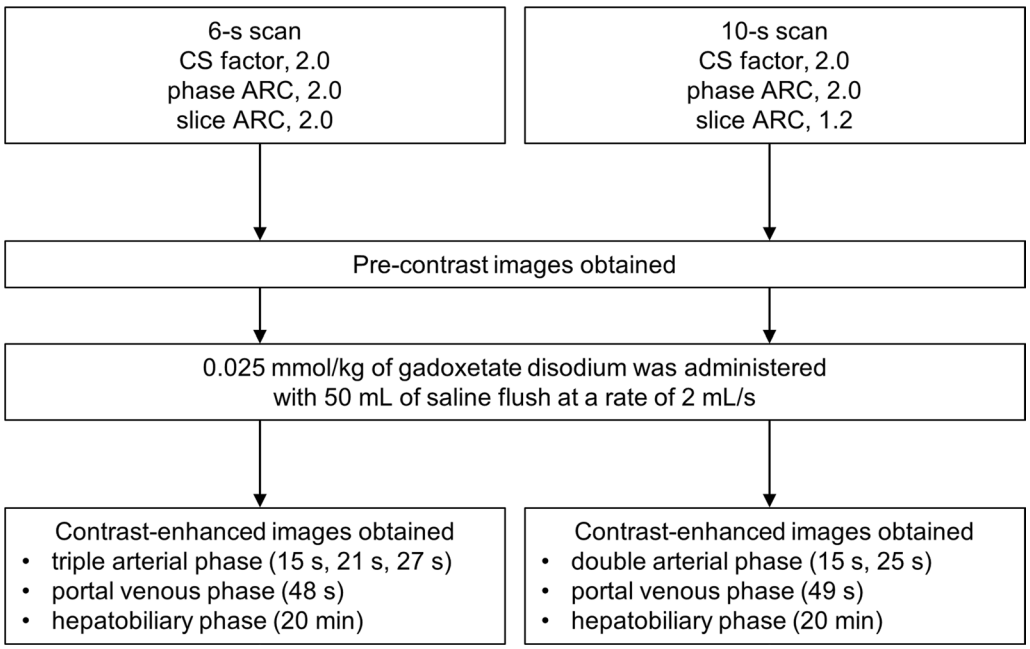

Fig. 1 Flow diagram for MR examinations in this study. The numbers in parentheses indicate the scan timing of contrast-enhanced phase after the start of contrast material injection

(RHA). In addition, the optimal arterial phase and overall image quality were also evaluated. The outline of the liver was assessed according to the following criteria: location, the posterior segment of the right hepatic lobe; level, the posterior segmental branch of the portal vein. The outline of the liver was assessed in all phases. IRHV was assessed in the pre-contrast and hepatobiliary phases. The right hepatic vein (RHV) was assessed if the IRHV could not be identified. As MR images of the posterior segment were considered to be less susceptible to motion artifacts caused by poor breath-holding and cardiac pulsation, RPV and RHA were assessed at the level of the posterior segmental branch of the portal vein. RPV was assessed in the portal venous phase, and RHA was assessed in multiple arterial phases. The overall VS and VS for the outline of the liver (Fig. 2), IRHV (Fig. 3), RPV (Fig. 4), and RHA (Fig. 5) were scored on a 4-point scale (1, poor; 2, relatively poor; 3, relatively good; and 4, good). Reference images for Figs. 2, 3, 4, and 5 were created using representative images of multiple participants. The reference images were selected from the MR images of participants included in this study, in which level and location were almost the same as evaluating images in this study. Reference images were created for the outline of the liver and IRHV for each phase to be evaluated. Optimal arterial phases were assessed in multiple arterial phases. VS of the optimal arterial phase was evaluated on a 5-point scale (1 = "too early," no enhancement of the hepatic artery and portal vein; 2 = "early," enhancement of the hepatic artery and no enhancement

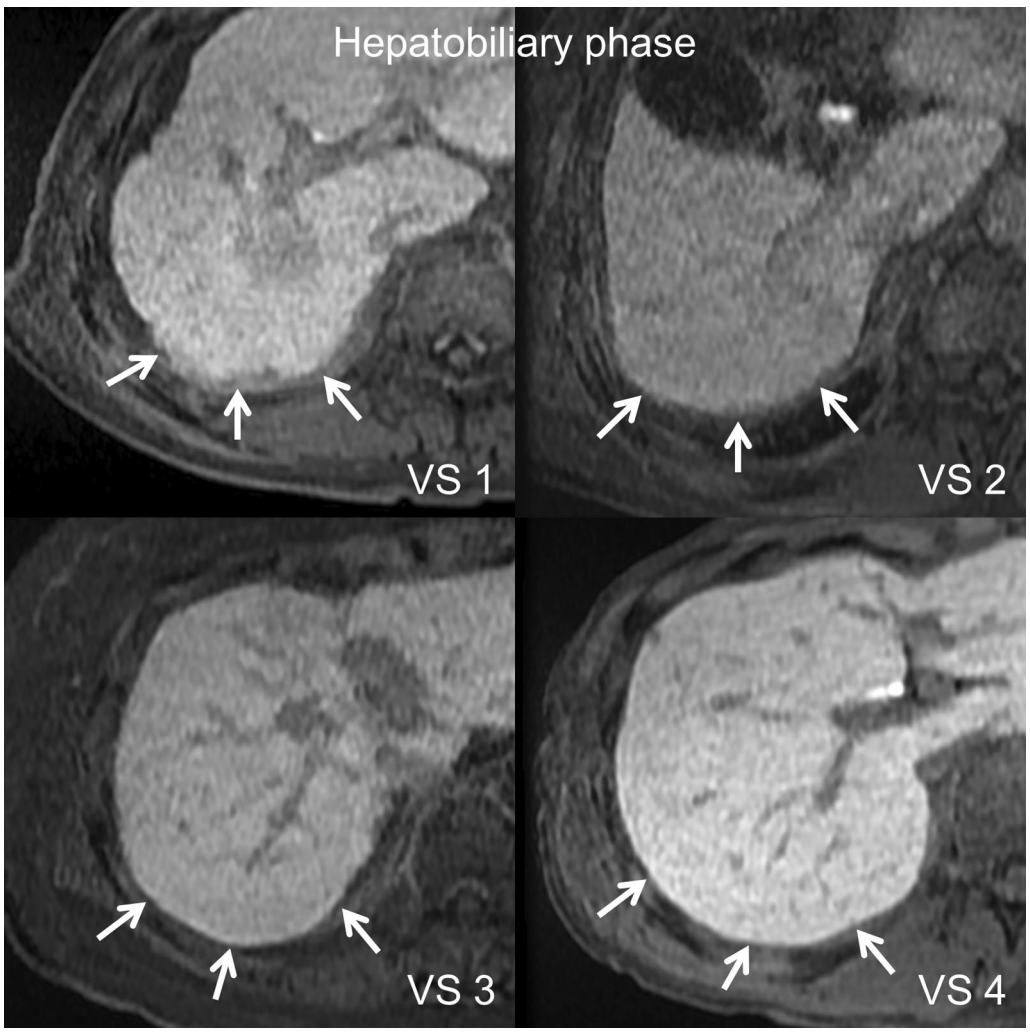

Fig. 2 Reference images for the assessment of the outline of the liver in the hepatobiliary phase. The outline of the liver was assessed posterior segment of the right hepatic lobe, at the level of the posterior segmental branch of the portal vein. White arrows show the outline of the liver being assessed

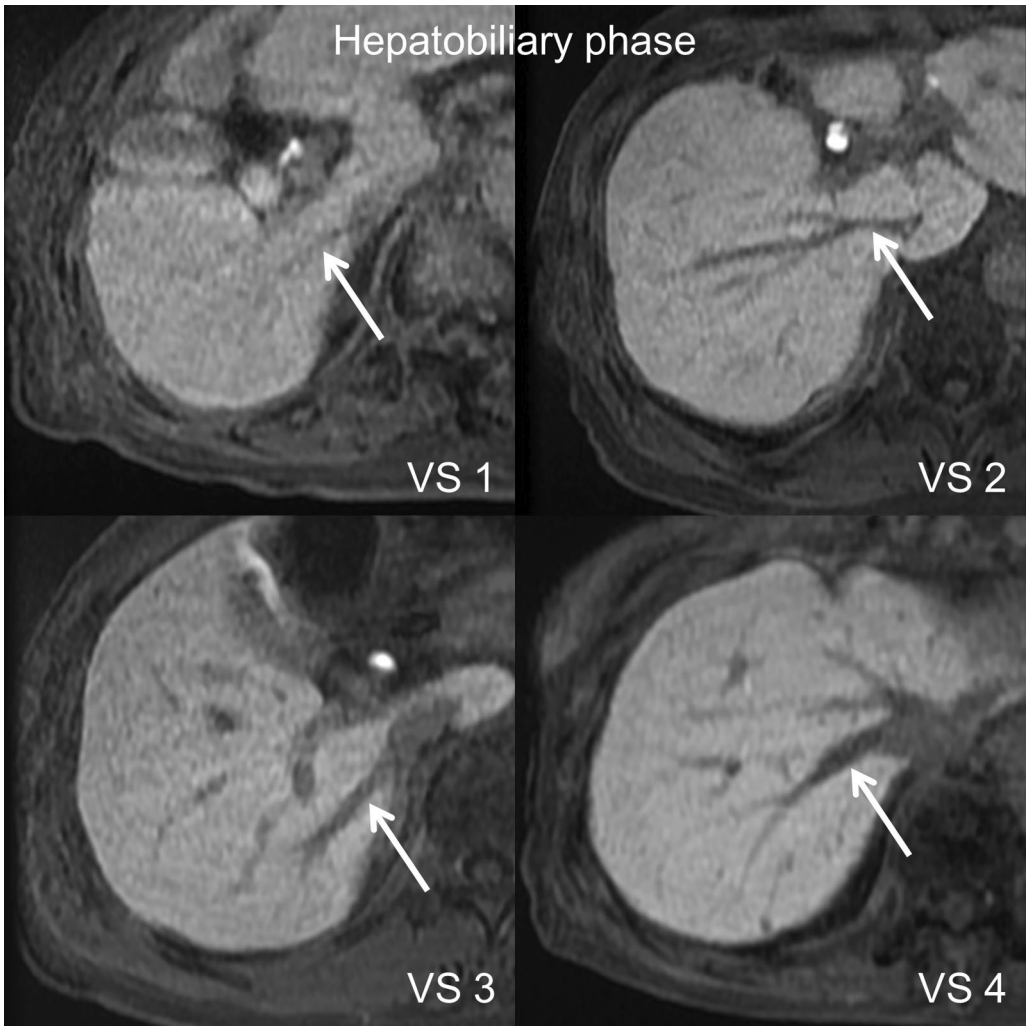

Fig. 3 Reference images for the assessment of the inferior right hepatic vein (IRHV) or right hepatic vein (RHV) in the hepatobiliary phase. The RHV was assessed if the IRHV could not be identified. White arrows show ITHV or RHV being assessed

of the portal vein; 3 = "optimal," enhancement of the hepatic artery and slight enhancement of the portal vein; 4 = "late," enhancement of the portal vein and liver parenchyma, no enhancement of the hepatic vein; 5 = "too late," enhancement of the liver parenchyma and hepatic veins). In evaluating overall image quality, MR imaging obtained with 6-s or 10-s scan protocols was evaluated in regard to whether it was sufficient for diagnostic imaging.

The VS determined by the two radiologists for each item, except for the optimal arterial phase, was averaged. The best VS score for the hepatic artery in multiple arterial phases was selected and averaged. The averaged VS was calculated by adding each VS of two readers and dividing by 2. It was difficult to decide the evaluation criteria with regard to overall image quality clearly; therefore, it was considered to be possible that there might be disagreements between two radiologists. Even if there were disagreements between two radiologists, we considered that it would be possible to assess the VS or image quality as a trend by averaging the VS of two radiologists.

Statistical analysis

The participant characteristics of the two scan groups were compared using the Chi-square test, Fisher's exact test, and *t*-test, as appropriate. For the quantitative evaluation, the SNRs of the multiple arterial and hepatobiliary phases were compared between the two groups using a *t*-test. For the qualitative evaluation, the average VS of the outline of the liver, IRHV, RPV, RHA, and overall image quality was compared between the two scan groups using the Mann–Whitney *U* test. The appropriateness of the arterial phase was assessed by determining the number of participants who received a score of 3 from both radiologists ("optimal" arterial phase). The suitability was

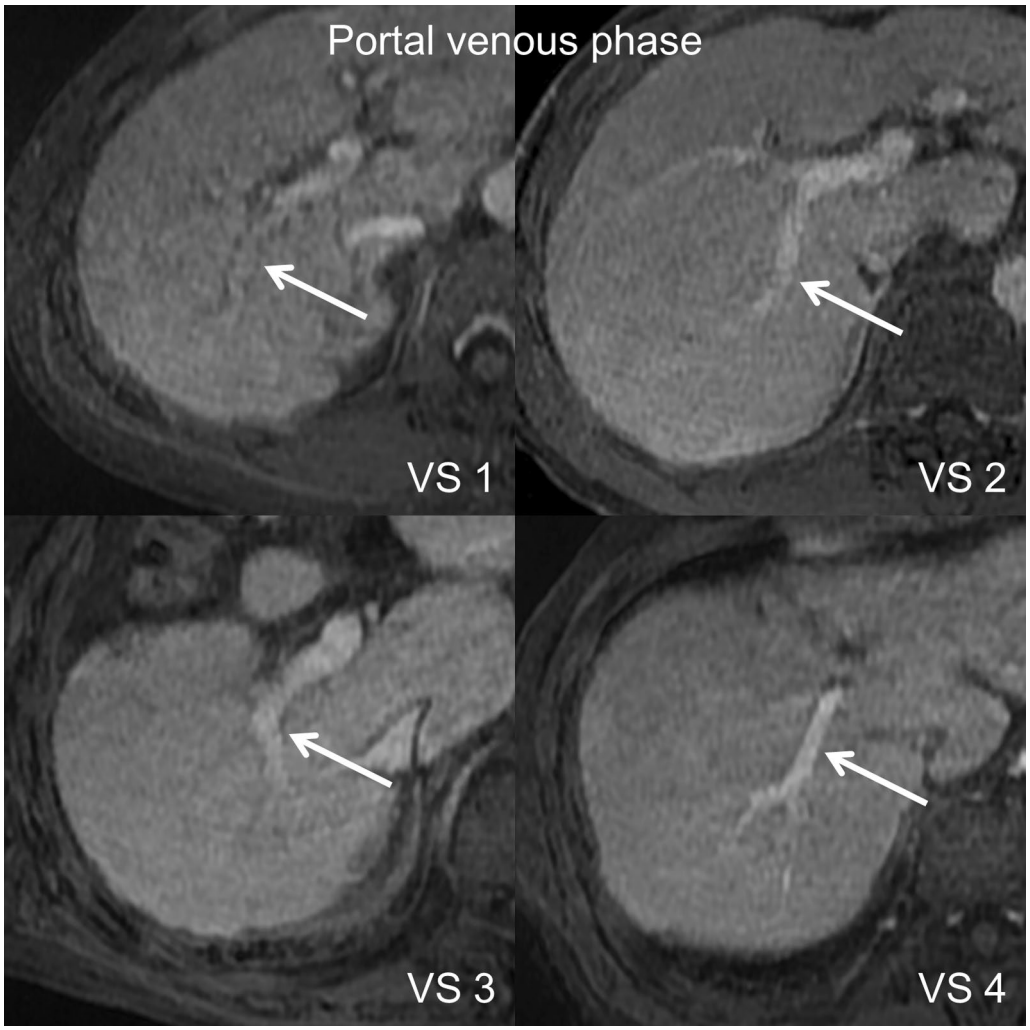

Fig. 4 Reference images for the assessment of the right portal vein (RPV). The right portal vein was assessed at the level of the posterior segmental branch. White arrows show RPV being assessed

compared between the two groups using the Chi-square test. Images with severe respiratory motion artifacts were excluded from the evaluation. Intraclass correlation coefficient (ICC) between the two radiologists was calculated for VS and optimal arterial phase. Statistical significance was set at a *P*-value < 0.05.

All statistical analyses were performed using EZR on R Commander Version 2.7-1 (Saitama Medical Center, Jichi Medical University, Saitama, Japan), which is a graphical user interface for R (The R Foundation for Statistical Computing, Vienna, Austria) [17].

Results

Figure 6 illustrates the flowchart of the participants and scan protocols in this study. Five participants, comprising three participants who had undergone blood tests > 3 months prior to the MRI examination and two participants who had undergone right hepatectomy, were excluded according to the exclusion criteria. Thus, 62 participants were enrolled in this study. The 6-s and 10-s scan groups comprised 46 and 22 participants, respectively. Six participants had undergone both 6-s and 10-s scans. Seventy-six MRI examinations were performed in this study. Fifty-one MRI examinations were performed in the 6-s scan group (28 males and 23 females; mean age, 70.8 ± 11.3; age range, 33–88 years) between September 2017 and February 2018. Five participants underwent 6-s scans twice during this period. Twenty-five MRI examinations were performed in the 10-s scan group (16 males and nine females; mean age, 69.1 ± 11.8; age range, 48–88 years) between May 2018 and October 2018. Three participants underwent 10-s scans twice during this period. Some participants underwent MRI examinations twice using the same protocol, because MR

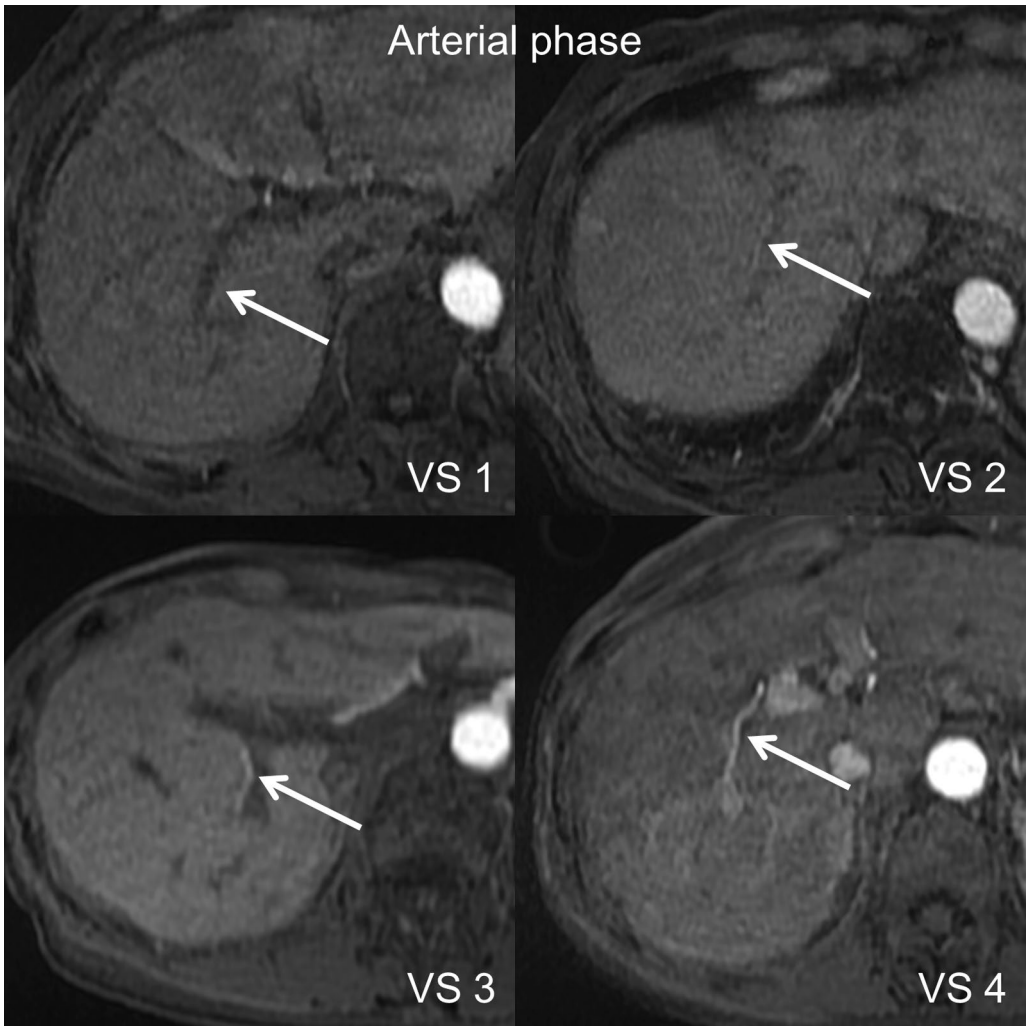

Fig. 5 Reference images for the assessment of the right hepatic artery (RHA). The right hepatic artery was assessed at the level of the posterior segmental branch of the right portal vein. White arrows show RHA being assessed

examinations were performed according to the requests of the attending physicians based on clinical course of the patient.

Table 2 summarizes the characteristics, including sex, age, body mass index, underlying liver disease, platelet count, total bilirubin levels, albumin levels, and ALBI score and grade, of the participants included in this study. No significant differences were observed between the two groups in terms of any of these characteristics.

Table 3 presents the SNRs of the liver for the multiple arterial and hepatobiliary phases in the two groups. No significant difference was observed between the two groups in terms of the SNR of the two phases ($P=0.593$ and 0.915 in the 6-s and 10-s scan groups, respectively).

Table 4 presents the VS and number of optimal arterial phases in the two groups. The average VS for the outline of the liver in the pre-contrast and arterial phases in the 10-s scan group was significantly higher than those in the 6-s scan group ($P=0.025$ and 0.039, respectively). Similarly, the average VS for IRHV in the pre-contrast phase in the 10-s scan group was significantly higher than that in the 6-s scan group ($P=0.035$). No significant difference was observed between the two groups in terms of the average VS for the following items: outline of the liver in the portal venous ($P=0.174$) and hepatobiliary ($P=0.287$) phases, IRHV in the hepatobiliary phase ($P=0.141$), RPV ($P=0.316$), and RHA ($P=0.545$). The probability of obtaining optimal arterial phase images was 56.9% and 48.0% in the 6-s and 10-s scan groups, respectively. No significant difference was observed between the two groups in terms of the appropriateness of the arterial phase ($P=0.731$). The average VS for overall image quality in the 10-s scan group was significantly higher than that in

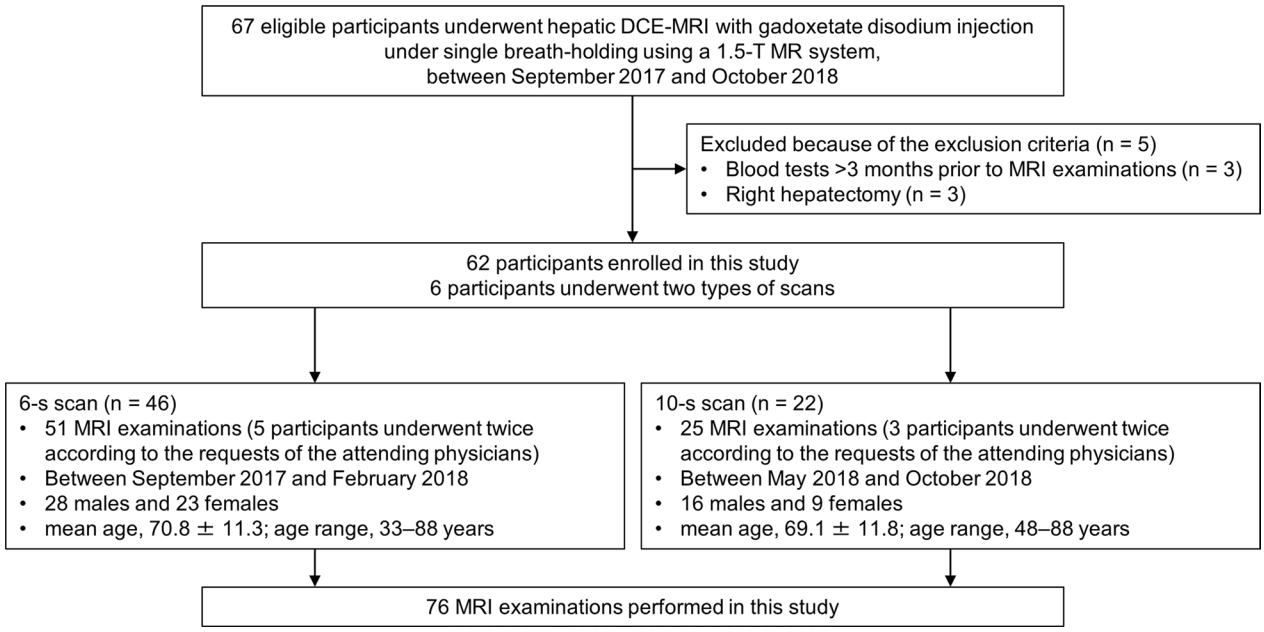

Fig. 6 Flowchart of the participants and scan protocols in this study

Table 2 Participant characteristics in the two groups

Characteristics	6-s scan group	10-s scan group	*P*-value
No. of examinations	51	25	Not applicable
Sex, M:F	28:23	16:9	0.612[a]
Age (years)	70.8 ± 11.3 (33–88)	69.1 ± 11.8 (48–88)	0.551[b]
BMI (kg/m^2)	22.4 ± 4.16 (14.2–33.3)	22.3 ± 3.82 (14.2–31.6)	0.659[b]
Background liver			0.643[c]
Chronic hepatitis B	8	5	0.888[a]
Chronic hepatitis C	22	10	0.990[a]
Alcohol	5	2	1[c]
Healthy liver	7	1	0.259[c]
Others[†]	9	7	0.459[a]
Platelet (× 10^4/μL)	13.7 ± 6.66 (4.3–30.7)	15.9 ± 7.82 (5.7–31.7)	0.212[b]
Total bilirubin (mg/dL)	1.03 ± 0.59 (0.4–2.87)	0.99 ± 0.54 (0.43–2.94)	0.755[b]
Albumin (g/dL)	3.91 ± 0.64 (2.3–5.2)	3.89 ± 0.49 (2.5–4.5)	0.871[b]
ALBI score	− 2.54 ± 0.63 (− 3.74 to − 1.11)	− 2.53 ± 0.48 (− 3.17 to − 1.2)	0.928[b]
ALBI grade, 1:2:3	31:16:4	14:10:1	

Data are presented as mean ± 1 standard deviation. The numbers in parentheses are the ranges

BMI, body mass index; ALBI, albumin–bilirubin

[a] Chi-square test

[b] *t*-test

[c] Fisher's exact test

[†] Others = non-B non-C, non-alcoholic steatohepatitis (NASH), primary biliary cholangitis (PBC), autoimmune hepatitis, and citrullinemia

Statistical significance was set at $P < 0.05$

the 6-s scan group ($P = 0.006$). Figures 7, 8, and 9 show representative images acquired using the two scan protocols. Figures 7 and 8 present the MR images acquired using the two scan protocols in the same patient. The average VS for the outline of the liver in the pre-contrast and arterial phases and the overall image quality

Table 3 Quantitative measurement values of the liver in the two groups

Phases and measurement items	6-s scan group	10-s scan group	*P*-value
Multiple arterial			
Mean signal intensity	799.41 ± 166.25 (394.25–1364.62)	767.57 ± 155.50 (481.55–1211.22)	0.275
SD	62.57 ± 18.91 (35.53–212.43)	60.18 ± 10.57 (39.55–92.40)	0.437
SNR	13.26 ± 3.05 (4.62–26.93)	12.98 ± 2.79 (7.20–19.16)	0.593
Hepatobiliary			
Mean signal intensity	1232.41 ± 260.40 (633.46–1962.09)	1235.61 ± 248.67 (803.34–1839.16)	0.961
SD	74.57 ± 16.80 (41.13–129.23)	74.29 ± 15.95 (42.16–110.99)	0.946
SNR	17.03 ± 4.21 (9.46–32.62)	17.14 ± 3.94 (9.64–25.85)	0.915

Data are presented as mean ± 1 standard deviation. The numbers in parentheses are the ranges

Statistical significance was set at $P < 0.05$

SD, standard deviation; SNR, signal-to-noise ratio

Table 4 Visual scores and number of optimal arterial phases

Evaluating items	6-s scan group	10-s scan group	*P*-value
Outline of the liver			
Pre-contrast	2.01 ± 0.81	2.28 ± 0.72*	0.025[a]
Arterial	2.10 ± 0.78	2.30 ± 0.62*	0.039[a]
Portal venous	2.43 ± 0.72	2.64 ± 0.56	0.174[a]
Hepatobiliary	3.04 ± 0.74	3.22 ± 0.76	0.287[a]
IRHV			
Pre-contrast	1.57 ± 0.67	1.88 ± 0.65*	0.035[a]
Hepatobiliary	2.09 ± 0.93	2.39 ± 0.79	0.141[a]
RPV	2.11 ± 0.75	2.28 ± 0.83	0.316[a]
RHA	2.25 ± 1.01	2.10 ± 0.90	0.545[a]
Optimal arterial phase	29/51 (56.9)	12/25 (48.0)	0.731[b]
Overall image quality	1.76 ± 0.66	2.22 ± 0.81*	0.006[a]

Data are presented as means ± 1 standard deviation, except for the optimal arterial phase, which shows the number of patients scored 3 ("Optimal" arterial phase) by both two radiologists

The numbers in parentheses are the percentage of the optimal arterial phase

IRHV, inferior right hepatic vein; RPV, right portal vein; RHA, right hepatic artery

[a] Mann–Whitney *U* test

[b] Chi-square test

*Significant difference ($P < 0.05$) between two scan protocols

for the 10-s scan protocol were improved compared with those in the 6-s scan protocol. The optimal arterial phase could not be obtained using the 10-s scan protocol; in contrast, the optimal arterial phase could be obtained using the 6-s scan protocol. The highest average VS for the overall image quality was achieved using the 10-s scan protocol (Fig. 9).

Table 5 presents the ICC between the two radiologists with regard to VS and optimal arterial phase. There was a good agreement in optimal arterial phase in 6-s scan group, and in IRHV of hepatobiliary phase, RPV, and optimal arterial phase in 10-s scan group. There was a slight-to-fair agreement in optimal arterial phase in IRHV of pre-contrast phase in 6-s scan group and in the outline of the liver in 10-s scan group.

Discussion

The present study demonstrated that the image quality in the 10-s scan group was significantly higher than that in the 6-s scan group. In a previous study with pre-contrast phase that included healthy volunteers, the image quality of the outline of the liver and IRHV in 6-s scan group was significantly decreased than reference standard obtained with 20-s scan, although decreasing of the image quality in 10-s scan group was not observed than reference standard obtained with 20-s scan. The image quality of the outline of the liver and IRHV was higher in the 10-s scan group compared with that in the 6-s scan group before the administration of the contrast agent. Although there is no reference standard obtained with 20-s scan in this study, this result is consistent with the findings of a previous study that included healthy volunteers [12]. No significant differences were observed between the images acquired in the portal and hepatobiliary phases (phases after contrast agent administration) in terms of the image quality based on the scan time. It has been reported that the image quality of a CS reconstruction image is determined by the quality of the acquired raw data, such as the SNR and sparsity [18, 19]. It was considered that the image quality before the administration of contrast agent in the 6-s scan group was degraded compared with that of the 10-s scan group owing to the lower tissue contrast caused by the decrease in data acquisition, lack of administration of contrast agent, lower SNR of the 1.5-T MRI system, and increased PI factor [18]. In contrast, no significant differences were observed in the SNRs of the hepatobiliary phase or the image quality of the portal and hepatobiliary phases between the two groups as the tissue contrast and SNR were increased owing to the administration of the contrast agent. The image quality

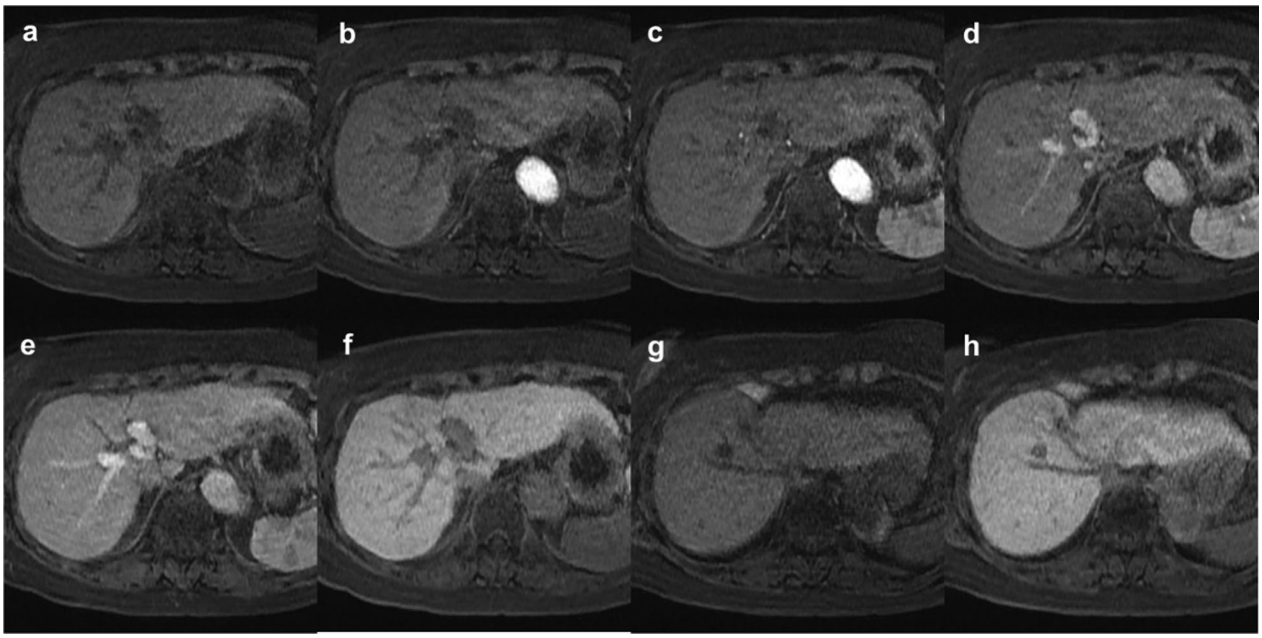

Fig. 7 Representative images of an 85-year-old female with chronic hepatitis B who underwent magnetic resonance imaging (MRI) using both protocols, same as the patient in Fig. 8. MR images acquired with the 6-s scan protocol (**a**, pre-contrast; **b**, first arterial phase; **c**, second arterial phase; **d**, third arterial phase; **e**, portal venous phase; **f**, hepatobiliary phase; **g**, pre-contrast; h, hepatobiliary phase) are shown. Images **a**–**f** were acquired at the level of the posterior segmental branch of the portal vein, whereas images **g** and **h** show the level of the right hepatic vein (RHV). The average visual score for each item is as follows: the outline of the liver (pre-contrast, 1.5; first arterial phase, 2.5; second arterial phase, 2.5; third arterial phase, 2; portal venous phase, 3; and hepatobiliary phase, 3.5); RHV (pre-contrast, 2 and hepatobiliary phase, 2); portal vein, 2.5; hepatic artery (first arterial phase, 1; second arterial phase, 2; and third arterial phase, 2); and overall image quality, 2. The optimal arterial phase was obtained in the third arterial phase

of the outline of the liver in the images acquired using the 10-s scan protocol in the arterial phase was significantly better, and no significant difference was observed between the two groups in terms of the SNR and VS of the hepatic artery. It was considered that the parenchyma of the liver was either not enhanced or only slightly enhanced in the early phase and that the tissue contrast was not increased; therefore, the image quality was degraded in the group with the shorter scan time. However, the hepatic artery was well-enhanced, and the tissue contrast was increased in the group with the shorter scan time [11, 20]. Furthermore, it has been reported that the high temporal resolution images depicted the real peak in SI during the arterial phase, and the average SI during the arterial phase was lower at a lower temporal resolution [21]. Therefore, although the scan time was shorter in the 6-s scan group, it was considered that the image quality was not degraded.

Several studies have demonstrated the clinical usefulness of double or triple arterial phase dynamic MR imaging in the detection of HCC, as it can acquire optimal arterial phase images [2–6]. The acquisition rates of the optimal arterial phase have been reported to be more than 70%, although scan protocols in references 20, 22 and 23 have been different from one of this study [20, 22, 23]. The acquisition rates of optimal arterial phase images using the two protocols in the present study were lower than those reported in previous reports, as the definition of optimal arterial phase images in this study (enhancement of the hepatic artery and "slight" enhancement of the portal vein, similar to the definition of the study by Agrawal et al.) has a narrower range for optimal arterial timing than previous reports except for the one by Agrawal et al. However, the acquisition rates of optimal arterial phase images using the two protocols in the present study were higher than those of conventional single arterial phase MRI [23]. Thus, the two protocols proposed in the present study could increase the acquisition rates of optimal arterial phase images in clinical practice. In the present study, the acquisition rates of optimal arterial phase images were higher in the 6-s scan group than those in the 10-s scan group; however, no significant difference was observed between the two groups in terms of the appropriateness of the arterial phase. It is possible that no significant difference was present owing to the small number of participants included in this study. Although no significant difference was observed in the SNR of the arterial phase, the image quality of the outline

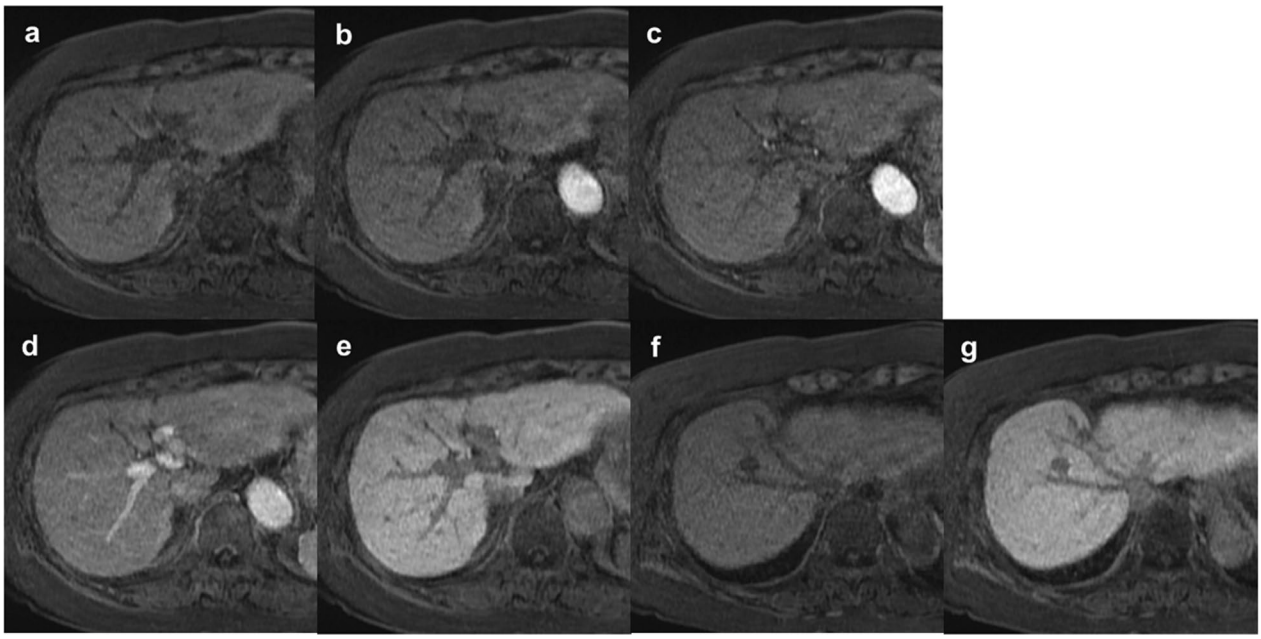

Fig. 8 Representative images of an 85-year-old female with chronic hepatitis B who underwent magnetic resonance imaging (MRI) using both scan protocols, same as the patient in Fig. 7. MR images acquired with the 10-s scan protocol (**a**, pre-contrast; **b**, first arterial phase; **c**, second arterial phase; **d**, portal venous phase; **e**, hepatobiliary phase; **f**, pre-contrast; **g**, hepatobiliary phase) are shown. Images **a**–**e** were acquired at the level of the posterior segmental branch of the portal vein, whereas images **f** and **g** show the level of the right hepatic vein (RHV). The average visual score for each item is as follows: the outline of the liver (pre-contrast, 3.5; first arterial phase, 2.5; second arterial phase, 2.5; portal venous phase, 3; and hepatobiliary phase, 3.5); RHV (pre-contrast, 2 and hepatobiliary phase, 2); portal vein, 3.5; hepatic artery (first arterial phase, 1 and second arterial phase, 2.5); and overall image quality, 2.5. The optimal arterial phase could not be obtained

of the liver in the arterial phase of the 10-s scan group was significantly better than that of the 6-s scan group. Better visualization of the outline of the liver plays an important role in the evaluation of hepatic fibrosis [24, 25]. Therefore, a 10-s scan (double arterial phase) protocol is recommended for multiple arterial phase DCE-MRI of the liver with gadoxetate disodium injection in combination with CS and PI under single breath-holding using a 1.5-T MR system. However, double arterial phase imaging has the risk of acquiring suboptimal arterial phase images for the evaluation of HCC, in addition to the reduction in the peak of early tumor stain owing to the lower temporal resolution than that of triple arterial phase imaging (higher temporal resolution) [21]. Therefore, it is important to set a scan delay after the administration of the contrast agent. For the same reason, it was considered that there was no significant difference between two scan groups in the VS of RPV".

The overall image quality in the 10-s scan group was significantly better than that in the 6-s scan group. Similarly, the image quality of several evaluation items was considerably better in the 10-s scan group. However, the average VS for the evaluation items in the 10-s scan group was lower than 3, indicating relatively poor image quality. In contrast, the average VS for the outline of the liver in the hepatobiliary phase was higher than 3 in the 10-s scan group (3.22), indicating relatively good image quality. This finding was attributed to the tissue contrast and SNR being highest in the hepatobiliary phase due to the uptake of the contrast agent by the hepatocytes. A 10-s scan protocol is recommended for high temporal resolution MR imaging of the liver with gadoxetate disodium injection in combination with CS and PI under single breath-holding using a 1.5-T MR system; however, its usefulness may be limited to particular situations, such as poor breath-holding, due to poor image quality. Shorter scan times reduce the incidence of motion artifacts [20, 26, 27]; thus, a 10-s scan protocol could be useful for the acquisition of hepatobiliary phase images for patients with poor breath-holding ability. The mean VS for the outline of the liver in the hepatobiliary phase was higher than 3, even in the 6-s scan group (3.04), and equal in both groups. Furthermore, no significant difference was observed between the two groups in terms of the SNR in the hepatobiliary phase. Therefore, the 6-s scan protocol can be especially useful in the above-mentioned situations.

The findings of the present study provide basic comparative information regarding the latest MR image reconstruction methods being considered for future clinical

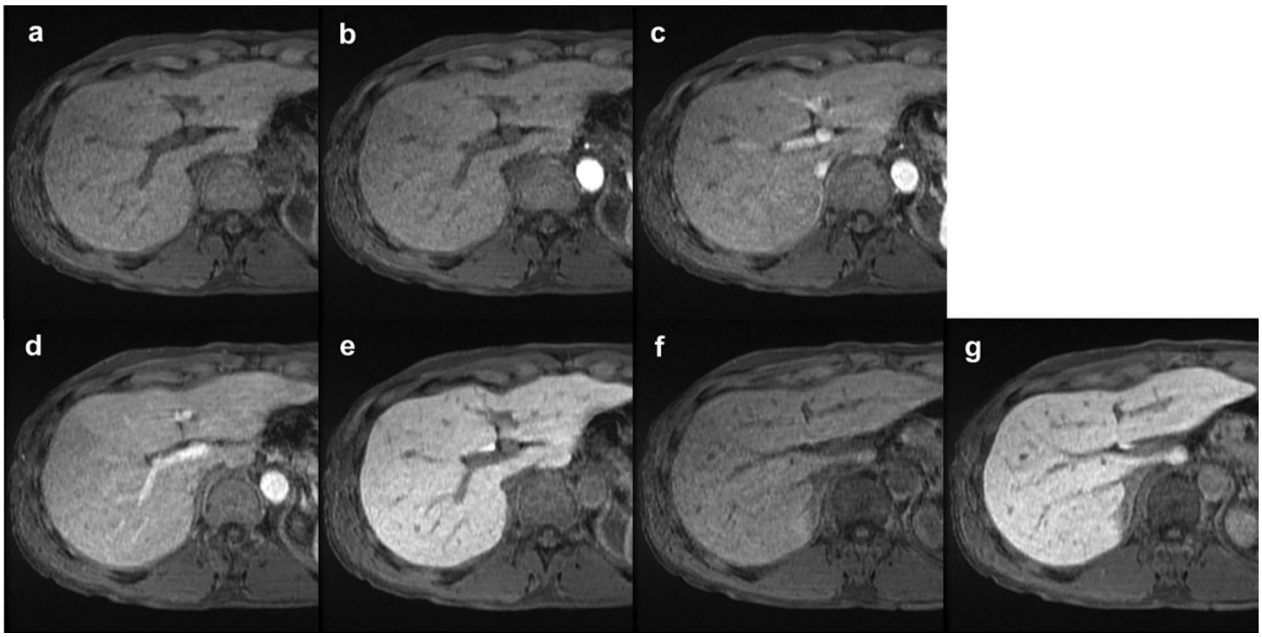

Fig. 9 Representative images of a 60-year-old male with citrullinemia. Magnetic resonance (MR) images acquired with the 10-s scan protocol (**a**, pre-contrast; **b**, first arterial phase; **c**, second arterial phase; **d**, portal venous phase; **e**, hepatobiliary phase; **f**, pre-contrast; and **g**, hepatobiliary phase) are shown. Images **a**–**e** were acquired at the level of the posterior segmental branch of the portal vein. Images **f** and **g** show the level of the inferior right hepatic vein (IRHV). The MR images acquired with the 10-s scan protocol demonstrate the highest visual score for overall image quality (an average visual score of 3.5). The average visual score for each item is as follows: the outline of the liver (pre-contrast, 3; first arterial phase, 2.5; second arterial phase, 2.5; portal venous phase, and 3; and hepatobiliary phase, 4); IRHV (pre-contrast, 1.5 and hepatobiliary phase, 2.5); portal vein, 2.5; and hepatic artery (first arterial phase, 1 and second arterial phase, 2). The optimal arterial phase was obtained in the second arterial phase

applications, such as deep learning reconstruction. The lack of knowledge regarding 1.5-T MR systems, especially in the field of abdominal imaging, is a major limitation. In the field of abdominal imaging, the 1.5 T MR system is widely used. However, 3-T MRI system is the mainstream in the field of abdominal imaging, and there are many reports of studies using 3-T MRI system. In making deep learning reconstruction algorithms, teaching data are necessary, but for the above reasons, teaching data in 1.5-T MRI system in abdominal imaging is few. The clinical significance of this study is high in this respect [28].

Table 5 Intraclass correlation coefficient between the two radiologists with regard to visual scores and optimal arterial phase

Evaluating items	6-s scan group	10-s scan group
Outline of the liver		
Pre-contrast	0.544	0.358
Arterial	0.588	−0.0184
Portal venous	0.492	0.238
Hepatobiliary	0.597	0.367
IRHV		
Pre-contrast	0.242	0.542
Hepatobiliary	0.695	0.74
RPV	0.628	0.773
RHA	0.573	0.44
Optimal arterial phase	0.744	0.802
Overall image quality	0.182	0.368

The present study has some limitations. First, the study population was small, and there was a difference in the number of participants between the two groups, which may have affected the results. Second, the diagnostic performance for the detection of liver diseases, such as HCC, was not evaluated. However, this was beyond the scope of this study, and the findings of the present study will aid in the evaluation of patients with liver disease in the future.

Conclusions

An acquisition time of 10 s is recommended for high temporal resolution DCE-MRI of the liver with gadoxetate disodium injection in combination with CS and PI under single breath-holding using a 1.5-T MR system. The 10-s scan protocol could be useful for hepatobiliary phase imaging in patients with poor breath-holding ability.

Abbreviations

ALBI	Albumin–bilirubin
ARC	Auto-calibrating reconstruction for Cartesian imaging
CS	Compressed sensing
DCE-MRI	Dynamic contrast-enhanced magnetic resonance imaging
GRE	Gradient recalled echo
HCC	Hepatocellular carcinoma
IRHV	Inferior right hepatic vein
LAVA	Liver acquisition with volume acceleration
MR	Magnetic resonance
PI	Parallel imaging
RHA	Right hepatic artery
RHV	Right hepatic vein
ROI	Regions of interest
RPV	Right portal vein
SD	Standard deviation
SI	Signal intensity
SNR	Signal-to-noise ratio
VS	Visual score

Acknowledgements
We would like to thank our colleagues at the Department of Radiology at Shinshu University for their cooperation. We would like to thank Honyaku Center Inc. for English language editing.

Author contributions
All authors contributed to the conception and design of the study. The data were acquired by FF, AS, MS, MT, HH, YK. Data analysis was performed by FF, FI, and AY. The first draft of the manuscript was written by FF and edited by AY and YF. All the authors have read and approved the final manuscript.

Funding
This study received no funding.

Availability of data and materials
All imaging data and assessment results were stored as electronic data. These data are available to the public upon request.

Declarations

Ethics approval and consent to participate
This study was conducted in accordance with the principles of the Declaration of Helsinki. The study protocol was approved by the institutional review board of Shinshu University (Matsumoto, Japan) on April 25, 2017 (approval number: 3040). Informed consent was obtained from all patients included in the study.

Consent for publication
Patients consented to the submission of the manuscript to the journal.

Competing interests
The authors have no conflicts of interest to declare relevant to the content of this article.

Author details
[1]Department of Radiology, Shinshu University School of Medicine, 3-1-1 Asahi, Matsumoto, Nagano 390-8621, Japan. [2]Division of Radiology, Shinshu University Hospital, 3-1-1 Asahi, Matsumoto, Nagano 390-8621, Japan.

Received: 26 October 2023 Accepted: 23 February 2024
Published online: 04 March 2024

References

1. Murakami T, Kim T, Takamura M, Hori M, Takahashi S, Federle MP, Tsuda K, Osuga K, Kawata S, Nakamura H, Kudo M (2002) Hypervascular hepatocellular carcinoma: detection with double arterial phase multi-detector row helical CT. Radiology 218:763–767. https://doi.org/10.1148/radiology.218.3.r01mr39763
2. Yoshioka H, Takahashi N, Yamaguchi M, Lou D, Saida Y, Itai Y (2002) Double arterial phase dynamic MRI with sensitivity encoding (SENSE) for hypervascular hepatocellular carcinomas. J Magn Reson Imaging 16:259–266. https://doi.org/10.1002/jmri.10146
3. Ito K, Fujita T, Shimizu A, Koike S, Sasaki K, Matsunaga N, Hibino S, Yuhara M (2004) Multiarterial phase dynamic MRI of small early enhancing hepatic lesions in cirrhosis or chronic hepatitis: differentiating between hypervascular hepatocellular carcinomas and pseudolesions. AJR Am J Roentgenol 183:699–705. https://doi.org/10.2214/ajr.183.3.1830699
4. Mori K, Yoshioka H, Takahashi N, Yamaguchi M, Ueno T, Yamaki T, Saida Y (2005) Triple arterial phase dynamic MRI with sensitivity encoding for hypervascular hepatocellular carcinoma: comparison of the diagnostic accuracy among the early, middle, late, and whole triple arterial phase imaging. AJR Am J Roentgenol 184:63–69. https://doi.org/10.2214/ajr.184.1.01840063
5. Yoon JK, Kim MJ, Lee S (2019) Compressed sensing and parallel imaging for double hepatic arterial phase acquisition in gadoxetate-enhanced dynamic liver magnetic resonance imaging. Invest Radiol 54:374–382. https://doi.org/10.1097/RLI.0000000000000548
6. Ikram NS, Yee J, Weinstein S, Yeh BM, Corvera CU, Monto A, Hope TA (2017) Multiple arterial phase MRI of arterial hypervascular hepatic lesions: improved arterial phase capture and lesion enhancement. Abdom Radiol 42:870–876. https://doi.org/10.1007/s00261-016-0948-8
7. Davenport MS, Viglianti BL, Al-Hawary MM, Caoili EM, Kaza RK, Liu PSC, Maturen KE, Chenevert TL, Hussain HK (2013) Comparison of acute transient dyspnea after intravenous administration of gadoxetate disodium and gadobenate dimeglumine: effect on arterial phase image quality. Radiology 266:452–461. https://doi.org/10.1148/radiol.12120826
8. Pietryga JA, Burke LM, Marin D, Jaffe TA, Bashir MR (2014) Respiratory motion artifact affecting hepatic arterial phase imaging with gadoxetate disodium: examination recovery with a multiple arterial phase acquisition. Radiology 271:426–434. https://doi.org/10.1148/radiol.13131988
9. Tanabe M, Higashi M, Iida E, Onoda H, Ihara K, Ariyoshi S, Kameda F, Miyoshi K, Furukawa M, Okada M, Ito K (2021) Transient respiratory motion artifacts in multiple arterial phases on abdominal dynamic magnetic resonance imaging: a comparison using gadoxetate disodium and gadobutrol. Jpn J Radiol 39:178–185. https://doi.org/10.1007/s11604-020-01042-z
10. Zhang T, Cheng JY, Potnick AG, Barth RA, Alley MT, Uecker M, Lustig M, Pauly JM, Vasanawala SS (2015) Fast pediatric 3D free-breathing abdominal dynamic contrast enhanced MRI with high spatiotemporal resolution. J Magn Reson Imaging 41:460–473. https://doi.org/10.1002/jmri.24551
11. Kawai N, Goshima S, Noda Y, Kajita K, Kawada H, Tanahashi Y, Nagata S, Matsuo M (2019) Gadoxetic acid-enhanced dynamic magnetic resonance imaging using optimized integrated combination of compressed sensing and parallel imaging technique. Magn Reson Imaging 57:111–117. https://doi.org/10.1016/j.mri.2018.11.004
12. Fukamatsu F, Yamada A, Hayashihara H, Kitou Y, Fujinaga Y (2021) Optimization of scan protocol for high temporal resolution magnetic resonance imaging of the liver under single breath-holding using compressed sensing and parallel imaging techniques in a 1.5-T magnetic resonance system. BJR Open 3:20210018. https://doi.org/10.1259/bjro.20210018
13. Chang KJ, Kamel IR, Macura KJ, Bluemke DA (2008) 3.0-T MR imaging of the abdomen: comparison with 1.5 T. Radiographics 28:1983–1998. https://doi.org/10.1148/rg.287075154
14. Ogura A, Miyati T, Kobayashi M, Imai H, Shimizu K, Tsuchihashi T, Doi T, Machida Y (2007) Method of SNR determination using clinical images. Jpn J Radiol Technol 63:1099–1104. https://doi.org/10.6009/jjrt.63.1099. (**in Japanese**)
15. Ogura A, Miyai A, Maeda F, Fukutake H, Kikumoto R (2003) Accuracy of signal-to-noise ratio measurement method for magnetic resonance images. Jpn J Radiol Technol 59:508–513. https://doi.org/10.6009/jjrt.KJ00003174111. (**in Japanese**)
16. Oshima S, Fushimi Y, Miyake KK, Nakajima S, Sakata A, Okuchi S, Hinoda T, Otani S, Numamoto H, Fujimoto K, Shima A, Nambu M, Sawamoto N, Takahashi R, Ueno K, Saga T, Nakamoto Y (2023) Denoising approach with deep learning-based reconstruction for neuromelanin-sensitive MRI: image quality and diagnostic performance. Jpn J Radiol. https://doi.org/10.1007/s11604-023-01452-9

17. Kanda Y (2013) Investigation of the freely available easy-to-use software 'EZR' for medical statistics. Bone Marrow Transplant 48:452–458. https://doi.org/10.1038/bmt.2012.244
18. Tamada D (2018) Implementation of compressed sensing for MR imaging. JJMRM 38:76–86. https://doi.org/10.2463/jjmrm.2018-1649. (**in Japanese**)
19. Breuer FA, Kannengiesser SA, Blaimer M, Seiberlich N, Jakob PM, Griswold MA (2009) General formulation for quantitative G-factor calculation in GRAPPA reconstructions. Magn Reson Med 62:739–746. https://doi.org/10.1002/mrm.22066
20. Ichikawa S, Motosugi U, Sato K, Shimizu T, Wakayama T, Onishi H (2021) Transient respiratory-motion artifact and scan timing during the arterial phase of gadoxetate disodium-enhanced MR imaging: the benefit of shortened acquisition and multiple arterial phase acquisition. Magn Reson Med Sci 20:280–289. https://doi.org/10.2463/mrms.mp.2020-0064a
21. Fujinaga Y, Ohya A, Tokoro H, Yamada A, Ueda K, Ueda H, Kitou Y, Adachi Y, Shiobara A, Tamaru N, Nickel MD, Maruyama K, Kadoya M (2014) Radial volumetric imaging breath-hold examination (VIBE) with k-space weighted image contrast (KWIC) for dynamic gadoxetic acid (Gd-EOB-DTPA)-enhanced MRI of the liver: advantages over Cartesian VIBE in the arterial phase. Eur Radiol 24:1290–1299. https://doi.org/10.1007/s00330-014-3122-0
22. Low RN, Bayram E, Panchal NJ, Estkowski L (2010) High-resolution double arterial phase hepatic MRI using adaptive 2D centric view ordering: initial clinical experience. AJR Am J Roentgenol 194:947–956. https://doi.org/10.2214/AJR.09.2507
23. Agrawal MD, Spincemaille P, Mennitt KW, Xu B, Wang Y, Dutruel SP, Prince MR (2013) Improved hepatic arterial phase MRI with 3-second temporal resolution. J Magn Reson Imaging 37:1129–1136. https://doi.org/10.1002/jmri.23920
24. Horowitz JM, Venkatesh SK, Ehman RL, Jhaveri K, Kamath P, Ohliger MA, Samir AE, Silva AC, Taouli B, Torbenson MS, Wells ML, Yeh B, Miller FH (2017) Evaluation of hepatic fibrosis: a review from the society of abdominal radiology disease focus panel. Abdom Radiol 42:2037–2053. https://doi.org/10.1007/s00261-017-1211-7
25. Higaki A, Kanki A, Yamamoto A, Ueda Y, Moriya K, Sanai H, Sotozono H, Tamada T (2023) Liver cirrhosis: relationship between fibrosis-associated hepatic morphological changes and portal hemodynamics using four-dimensional flow magnetic resonance imaging. Jpn J Radiol 41:625–636. https://doi.org/10.1007/s11604-023-01388-0
26. Zaitsev M, Maclaren J, Herbst M (2015) Motion artifacts in MRI: a complex problem with many partial solutions. J Magn Reson Imaging 42:887–901. https://doi.org/10.1002/jmri.24850
27. Cui L, Song Y, Wang Y, Wang R, Wu D, Xie H, Li J, Yang G (2023) Motion artifact reduction for magnetic resonance imaging with deep learning and k-space analysis. PLoS ONE 5(18):e0278668. https://doi.org/10.1371/journal.pone.0278668
28. Yamada A, Kamagata K, Hirata K, Ito R, Nakaura T, Ueda D, Fujita S, Fushimi Y, Fujima N, Matsui Y, Tatsugami F, Nozaki T, Fujioka T, Yanagawa M, Tsuboyama T, Kawamura M, Naganawa S (2023) Clinical applications of artificial intelligence in liver imaging. Radiol Med 128:655–667. https://doi.org/10.1007/s11547-023-01638-1

Publisher's Note